Stem Cell Research & Therapy

RESEARCH

Open Access

Glutamine-αKG axis affects dentin regeneration and regulates osteo/odontogenic differentiation of mesenchymal adult stem cells via IGF2 m6A modification

Qinglu Tian[1], Shiqi Gao[3], Siying Li[1], Mian Wan[2], Xin Zhou[1], Wei Du[2], Xuedong Zhou[2], Liwei Zheng[1*] and Yachuan Zhou[2*]

Abstract

Background Multi-lineage differentiation of mesenchymal adult stem cells (m-ASCs) is crucial for tissue regeneration and accompanied with metabolism reprogramming, among which dental-pulp-derived m-ASCs has obvious advantage of easy accessibility. Stem cell fate determination and differentiation are closely related to metabolism status in cell microenvironment, which could actively interact with epigenetic modification. In recent years, glutamine-α-ketoglutarate (αKG) axis was proved to be related to aging, tumorigenesis, osteogenesis etc., while its role in m-ASCs still lack adequate research evidence.

Methods We employed metabolomic analysis to explore the change pattern of metabolites during dental-pulp-derived m-ASCs differentiation. A murine incisor clipping model was established to investigate the influence of αKG on dental tissue repairment. shRNA technique was used to knockdown the expression of related key enzyme-dehydrogenase 1(GLUD1). RNA-seq, m6A evaluation and MeRIP-qPCR were used to dig into the underlying epigenetic mechanism.

Results Here we found that the glutamine-αKG axis displayed an increased tendency along with the osteo/odontogenic differentiation of dental-pulp-derived m-ASCs, same as expression pattern of GLUD1. Further, the key metabolite αKG was found able to accelerate the repairment of clipped mice incisor and promote dentin formation. Exogenous DM-αKG was proved able to promote osteo/odontogenic differentiation of dental-pulp-derived m-ASCs, while the inhibition of glutamine-derived αKG level via GLUD1 knockdown had the opposite effect. Under the circumstance of GLUD1 knockdown, extracellular matrix (ECM) function and PI3k-Akt signaling pathway was screened out to be widely involved in the process with insulin-like growth factor 2 (IGF2) participation via RNA-seq. Inhibition of glutamine-αKG axis may affect IGF2 translation efficiency via m6A methylation and can be significantly rescued by αKG supplementation.

*Correspondence:
Liwei Zheng
liwei.zheng@scu.edu.cn
Yachuan Zhou
zhouyc@scu.edu.cn
Full list of author information is available at the end of the article

Conclusion Our findings indicate that glutamine-αKG axis may epigenetically promote osteo/odontogenic differentiation of dental-pulp-derived m-ASCs and dentin regeneration, which provide a new research vision of potential dental tissue repairment therapy method or metabolite-based drug research.

Keywords ASCs, Glutamine-αKG Axis, Mesenchymal stem cells, Dentin regeneration, IGF2, Epigenetic

Background

Tooth hard tissue regeneration has been one of the key point and breakthrough field of dental diseases treatment including caries, dental trauma, tooth development defects (enamel and dentin) etc. Traditional dental treatment methods towards these clinical symptoms are usually based on material-assisted restoration and infection control. However, as the development of biological therapy, spontaneous tissue regeneration and repair have become the targets of treatment, meanwhile several dental-derived stem cells gradually came into view. As a typical type of dental-pulp-derived mesenchymal adult stem cells (m-ASCs) [1, 2], dental pulp stem cells (DPSCs) have been studied and verified as owning high capacity of multilineage differentiation and described as an alternative to pluripotent stem cells [3–5]. Compared with other pluripotent stem cells, easier accessibility endows DPSCs better opportunity and applicability for tissue engineering and stem cell therapy [4, 5]. Currently, most DPSCs-based dentin regeneration explorations focused on materials as scaffold like nanocomposite [6], 3D-bioprinting material [7] etc., while DPSCs as "seeds". However, throughout the entire regeneration and repair process, biological scaffolds can be considered as a "static" factor, but the activities and biological behaviors of cells in the microenvironment are "dynamic". Metabolites in cell microenvironment are typical "dynamic" factors, which haven't been taken seriously until recent years. In-depth studies on metabolite in regulating the activity and biological behavior of stem cells are necessary.

During lineage differentiation of ASCs, their metabolic characteristics undergoes corresponding reprogramming. Glutamine is an important metabolite for carbon and nitrogen supply as one of the most abundant amino acids, which can reach a 40% free amino acid proportion in the blood vessels of muscle tissue [8]. αKG is a key metabolite in glutamine metabolism and has other names like 2-ketoglutaric acid or 2-oxoglutaric acid, acting as an intersection between glucose and glutamine metabolism [9, 10].The glutamine-αKG axis was noticed for its indispensable role of cell growth and the crosstalk function between amino acid metabolism and energy metabolism [8, 11, 12]. Glutamine can be metabolized to produce glutamate under the catalysis of glutaminase (GLS). Furthermore, with NADP + /NAD + as coenzyme, glutamate can be reversibly metabolized into αKG under the catalysis reaction conducted by glutamate dehydrogenase (GLUD), accompanied by the release of ammonia and the production of NADPH/NADP via oxidation–reduction reaction. αKG-related metabolism epigenetically modulates stem cells fate, influences tumorigenesis, cell differentiation and cell senescence [13, 14]. Study have shown that increased intracellular αKG level is conducive to the self-renewal of embryonic stem cells and αKG can also accelerate the early differentiation of primary human pluripotent stem cells [15]. The glutamine-αKG metabolic axis mainly refers to the reversible metabolic pathway through which glutamine is ultimately metabolized to produce αKG under the action of related enzymes [11]. Although human dental pulp stem cells(hDPSCs) has been verified to closely related to several metabolic activities [16–18], the role of glutamine-αKG axis in hDPSCs differentiation was still lack of adequate research evidence.

Epigenetics refers to the phenomenon that due to changes in the external environment, related phenotypes or biological traits can be inherited without altering the DNA sequence via regulating the methylation, acetylation or other epigenetic modifications of proteins, DNA, or RNA. Since twentieth century, as the mysterious veil of genetic landscape was gradually revealed, epigenetics has become a hot research field in recent years. Environmental factors, especially some metabolic products and activities closely related to cellular life activities, play an undeniable "bridge" role in connecting the micro world within cells with the external macro environment [19]. Moreover, recent studies have shown that epigenetic modifications are important influencing factors and regulatory mechanisms in determining the fate of stem cells in related studies on the mechanisms of action and potential applications of stem cells [20, 21].

Here, we intended to explore the potential effect and epigenetic mechanism involvement of glutamine-αKG metabolic axis on osteo/odontogenic differentiation of human dental pulp stem cells (hDPSCs).

Methods

Primary human dental pulp stem cells culture and odontogenetic differentiation

After obtaining the patient's informed consent, human dental pulp cells (hDPSCs) were obtained and cultured from 20 healthy caries-free third permanent molars

and premolars (extracted due to orthodontic demand), extracted from patients aged 18 ~ 30 years from the outpatient department of oral and maxillofacial surgery of West China Stomatology Hospital of Sichuan University during 2022.1 to 2023.1. Passage 3 hDPSCs were used in all experiments. Cells were seeded in six-well plates at a density of 1×10^5 cells per well and cultured in DMEM containing 10% FBS and 1% Penicillin–streptomycin mix until they reached 80% confluence. The medium was then replaced with osteo/odontogenic differentiation medium containing DMEM supplemented with 10% FBS, 50 μg/mL ascorbic acid, 10 mM β-glycerophosphate, and 10^{-7} mol /L dexamethasone.

Flow cytometry

hDPSCs were collected on 7D and 14D after osteogenic induction, washed with PBS and resuspended using 5%BSA (Biofroxx, Germany). as staining buffer. Then Fixation/Permeabilization Kit (Cat #554,714, BD Biosciences, USA) was used to fix the single cell suspension for 30 min and washed with Perm/Wash buffer for 3 times. Two-step indirect staining protocol was performed using first antibody and second antibody incubating for 40 min and 30 min respectively at 4 °C. After washing with Perm/Wash buffer for 3 times, cells were additionally for dead cell exclusion. The data was performed and acquired on Attune NXT flow cytometer (Thermo Fisher Scientific, USA) and data was analyzed by Flowjo software. The primary antibodies included anti-CD29 (Cat. #303,003, BioLegend, USA), anti-CD90 (Cat. #328,109, BioLegend, USA), anti-CD34 (Cat. #343,603, BioLegend, USA), anti-CD45 (Cat. #368,509, BioLegend, USA).

RNA extraction and qPCR

Total RNA was extracted using TRIzol (Invitrogen, USA). The cDNA synthesis was performed with HiScript III qRT SuperMix (Vazyme, Nanjing, China). The qRT- PCR reactions were prepared with SYBR Green (Vazyme, Nanjing, China) following the manufacturer's protocols.

Alkaline phosphatase activity analysis and Alizarin red S staining

After 7 days and 14 days of incubation, the cells of each group were rinsed three times with PBS (pH 7.4) and fixed in 4% paraformaldehyde (Cat#P0099, Beyotime, China) for 15 min at room temperature. For alkaline phosphatase (ALP) and Alizarin Red staining (ARS), an ALP assay kit (Cat#P0321S, Beyotime, China) and alizarin red staining reagent (Cat #C0140, Beyotime, China) were used according to the manufacturer's instructions. Images were observed and photographed using a stereomicroscope (Olympus, Japan).

Untargeted and targeted metabolomics analysis

Metabolomics analysis was performed by APPLIED PROTEIN TECHNOLOGY Inc. (Shanghai, China). Untargeted metabolomics methods in this research were based on ultra-high performance liquid chromatography coupled with Quadrupole-time of flight mass spectrometry (UHPLC-Q-TOF MS), while targeted metabolomics methods were based on multiple reaction monitoring (MRM) technique. Agilent 1290 Infinity LC Liquid Chromatography was used in MS process.

Animals

Thirty male specific pathogen-free (SPF) C57BL/6 mice, 4-weeks-old, were obtained from Chengdu GemPharmatech Co., Ltd. The mice were housed at the State Key Laboratory of Oral Diseases, West China Hospital of Stomatology, Sichuan University. They were kept in an environment with a temperature maintained at 22 °C and a 12-h light/dark cycle. The animal study was conducted in accordance with the ARRIVE guidelines 2.0.

Incisor clipping and fluorescence double-labeling animal model

A mouse incisor clipping model was used to explore the role of αKG in tooth acute injury and dentin formation. 4-weeks-old male C57 mice were fed with 0.25% (w/v) αKG-containing water for two weeks. After proper anesthesia with intraperitoneal injection of pentobarbital (1 mg/kg, Sigma-Aldrich, USA), left incisor was clipped. In the measuring model, a notch was made near gingival margin of mice incisors using dental bar, while the notch movements were measured 3 days after clipping compared to the unclipping side. Animals were euthanized with an intraperitoneal injection for pentobarbital overdose (about 400 ~ 500 μl). 6-weeks-old old mice were sacrificed 3 days after clipping to collect samples and data. In the fluorescence double-labeling model, 1 mg/ml calcein (Cat. #C0857, Sigma, USA) was intraperitoneally injected as soon as the clipping was performed on clipping day 0(D0), 2 mg/ml Alizarin Complexone dihydrate (Cat. #A861758, Macklin, China) was intraperitoneally injected as well on the third day after clipping (D3), and finally the samples were collected on the fourth day after clipping (D4).

Western Blot

Protein extraction was performed by Whole cell Lysis Assay Kit (Cat. #KGP250, Keygens BioTECH, China) in accordance with manufacturer's protocols. Cells or tissues were lysated in lysis buffer containing protease and phosphatase inhibitor cocktail. Protein concentration was determined by BCA Protein Quantitative Kit (Cat.

#P0010, Beyotime, China) and separated by SDS-PAGE electrophoresis (Bio-Rad, USA), immunoblotted with the indicated antibodies. Relative quantifications of protein were analyzed using Image J software (Version 1.8.0). Full length blots are presented in Additional file 1: Fig. S1A-C.

Immunofluorescence/Immunochemistry Staining Assay

The separated mandibular was embedded in paraffin in sagittal position and cut for 4 μm sections by Leica slicer (Leica, Germany). The antigen retrieval condition was 99 °C for 20 min. The samples were blocked and permeabilized with TBST containing 5% BSA at room temperature for 1 h, and then incubated overnight at 4 °C with the primary antibodies, which were diluted in TBST containing 5% BSA. The primary antibodies include anti-Ki67 (ab279653, Abcam, USA) and anti-GLUD1(Cat. # sc-515542, Santa Cruz Biotechnology, USA). The secondary antibody, goat anti-mouse Alexa 488(Cat.# ab150113, Abcam, USA), was added and incubated at room temperature for 1 h. Nuclei were stained with DAPI (Cat# GDP024, Servicebio, China). Images were captured with confocal scanning microscope (Olympus, Japan).

Masson's trichrome staining assay

The separated mandibular was embedded in paraffin in sagittal position and cut for 4 μm sections by Leica slicer (Leica, Germany). The Masson staining process was carried out by Masson's Trichrome Stain Kit (Cat. #G1340, Solarbio, China) in accordance with manufacturer's protocols.

αKG level evaluation

hDPSCs were collected on 7D and 14D after osteo/odontogenic induction. The evaluation of αKG was carried out by α-Ketoglutarate Assay Kit (Cat. #MAK054, Sigma, USA) in accordance with manufacturer's protocols.

m6A level evaluation

The evaluation of m6A was carried out by EpiQuick m6A RNA Methylation Quantification Kit (Cat. #P-9005, Epigentek, USA) in accordance with manufacturer's protocols.

RNA-seq

Total RNA was extracted using Trizol reagent (Invitrogen, USA) following the manufacturer's procedure, and high-quality RNA samples with RIN number > 7.0 were used to construct sequencing library. The average insert size for the final cDNA libraries were 300 ± 50 bp. 2 × 150 bp paired-end sequencing (PE150) was performed on an Illumina Novaseq™ 6000 (LC-Bio technology CO., Ltd., Hangzhou, China) following the vendor's recommended protocol. Information about gene set used in GSEA analysis referenced GSEA website (https://www.gsea-msigdb.org/gsea/index.jsp). Information about KEGG pathways referenced KEGG website (https://www.kegg.jp).

MeRIP-qPCR

MeRIP-Seq was performed by Gene Create Inc. (Wuhan, China). Briefly, total RNA was extracted using TRIzol (Invitrogen, USA). The MeRIP assay was carried out by the GenSeqTM m6A RNA IP Kit (Cat. # GS-ET-001GenSeq, China) in accordance with manufacturer's protocols. Modification of m6A towards target genes was determined by RT-qPCR with specific primers (Additional file 2: Table S1).

Data analysis

Statistical analysis was performed using GraphPad Prism 9.5.1 (GraphPad Software Inc., San Diego, CA). Independent unpaired two-tailed Student' s t tests and paired two-tailed Student' s t tests were used for comparing between two groups. Comparisons between multiple groups were assessed by one-way ANOVA with Tukey's multiple comparisons test. All in vitro experiments were carried out in at least three replicates and the data presented are from one representative experiment, and $p < 0.05$ was considered statistically significant.

Results

Glutamine-αKG axis displays a dynamic pattern during osteo/odontogenic differentiation of hDPSCs

Dental-pulp-derived hDPSCs were isolated, cultured, and identified according to method described above (Fig. 1A-D). Flow cytometry was performed to identify the surface markers of mesenchymal stem cells, which is positive for CD29, CD90 and negative for CD45, CD34 (Fig. 1B) [22]. The osteo/odontogenic induction of hDPSCs was confirmed successful via ARS and ALP staining, while the osteo/odontogenic markers including COL1, DMP1, OCN, OSX, RUNX2, ALP and DSPP showed and upward tendency along with differentiation. A joint analysis on non-targeted metabolomics and targeted metabolomics data was then conducted to analyze the pattern of glutamine-αKG axis on D0, D1, D7 after hDPSCs osteo/odontogenic inducing (Fig. 1E-I). Most metabolites were upregulated along with differentiation as the volcano plot displayed on both D1 and D7 compared to D0 (Fig. 1E and Additional file 1: Fig. S2A). The metabolic atlas of amino acid related metabolites gradually increased (Fig. 1F). The level of L-Glutamine and L-Glutamate elevated during the early osteo/odontogenic differentiation (Fig. 1G), and the most importantly, level of αKG increased along with osteo/odontogenic differentiation significantly (Fig. 1H). Meanwhile, NAD^+, NADH,

$NADP^+$, NADPH, ADP, ATP presented an upward tendency as well, suggesting an active ATP production and energy metabolism to meet the end of great energy demand during differentiation (Additional file 1: Fig. S2B).

There are mainly three metabolic path that glutamine being metabolized into αKG, distinguished by three enzyme including GLUD,GPT,and GOT (Additional file 1: Fig. S2C), among which the GLUD-mediated axis was reported to be the canonical one [8]. To verify the necessity of glutamine-αKG axis, hDPSCs were firstly cultured in cell culture medium without glutamine (-Gln group) to interfere with the level of intracellular αKG since the source of amino acid pathway is blocked. Compared with normal mineralization group (control group), -Gln group presented less Alizarin red positive mineralized nodules and lower ALP activity, which can be rescued by 2 mM DM-αKG and 4 mM DM-αKG (Fig. 1J-K). Meanwhile, the qPCR results of ALP and RUNX2 presented a reducing tendency in -Gln group. Intriguingly, administration of different concentration of DM-αKG to -Gln group partially rescued the inhibition of osteo/odontogenic differentiation on D14 (Fig. 1L). And it should be noted that hDPSCs in -Gln group grew poorly.

αKG accelerates the growing speed of rodent clipped incisor and dentin formation around cervical loop (CL)

To investigate the potential effect of αKG on dentin formation under both normal tooth development and injury status, we chose mice incisor to establish an acute tooth injury model and focused on cervical loop (CL) to observe the effect of αKG on rodent incisor (Additional file 1: Fig. S3A). After administration of 0.25% αKG in drinking water, the growing speed of clipped incisor was significantly improved (Additional file 1: Fig. S3B). Previous studies reported that clipping may promote proliferation status around CL and propel the mesenchymal stem cell into a quicker renewal condition to speed up dental tissue reparation [23–25]. In this clipping model, $Ki67^+$ cells appeared on top of the LaCL at clipping-D3 compared to clipping-D0 (Fig. 2A), which might indicating the supplement of consumed proliferating cells towards dental epithelial stem cells (DESCs), in accordance with previous report [23]. Apart from LaCL, we also observed increased Ki67 expression after clipping on D3 in neurovascular bundle (NVB), a region with high-density blood vessels and nerves in dental pulp and indispensable for mesenchymal development and dentine formation (Fig. 2A).To further explore the mineral matrix deposition around the cervical loop (CL) quantitatively, we established a fluorescence double-labeling model (Fig. 2B-C). The results came out that additional αKG supplement speed up the growing speed in both clipping and non-clipping group (Fig. 2D, F). Besides, the clipping side of incisor grows faster than the non-clipping side in both control group and 0.25%(w/v) αKG group (Fig. 2D, G). We used paired t-test to exclude the potential influence of self-abrasion and self-growing on statistical analysis (Fig. 2G). The clipping side incisor of αKG group presented the highest growing speed of 569.4 μm/24 h (Additional file 1: Fig. S3C). The immunofluorescent staining revealed that Ki67-positive dental pulp cells significantly mount up in 0.25%(w/v) αKG group under both non-clipping and clipping status, indicating the high-speed renewal of dental pulp stem cell pool (Fig. 2E). Moreover, via Masson's trichrome staining assay, we observed that both αKG and clipping can bring the dentin deposition point forward significantly (Fig. 2H-I). The Vickers hardness of dentin around CL region significantly decreased under the application of αKG (Fig. 2J-K). This may also imply a more active deposition of poor-mineralized pre-dentin in 0.25%(w/v) αKG group. However, the Vickers hardness of dentin around incisal region showed no significant difference (Fig. 2K). The effect of αKG on incisor repairment and cervical loop was illustrated as sketch map (Fig. 2L). Under the circumstance of αKG supplementation, enhanced and activated proliferation state may partial attribute to the speed-up incisor formation and earlier dentin deposition point.

αKG promotes osteo/odontogenic differentiation of hDPSCs

For further exploration, exogenous αKG was added to cell culture medium to figure out the potential influence of

(See figure on next page.)

Fig. 1 Metabolomics analysis of hDPSCs during early osteo/odontogenic differentiation on D0, D1, D7. **A** Cultivate morphology of hDPSCs (Passage 0). **B** Identification of hDPSCs' surface markers (CD90, CD29, CD45 CD34) by flow cytometry. **C** ARS and ALP staining of hDPSCs during osteo/odontogenic induction. **D** qPCR results of osteo/odontogenic related genes. **E** Volcano plot (D0 vs D1, D0 vs D7). The highlighted pink points refer to statistically significantly metabolites($p < 0.05$). **F** Heatmap of "amino acids, peptides, and analogues" on D0, D1 and D7. **G–H** Sketch picture of glutamine-αKG axis along with boxplot of key metabolites including L-Glutamine, L-Glutamate and αKG (One-way ANOVA was performed) ($p < 0.01$). (L-Glutamine and L-Glutamate levels were evaluated via untargeted metabolomics methods, and αKG level was confirmed via targeted metabolomics methods). **I** Circular heatmap of energy metabolism related metabolites on D0, D1 and D7. **J** ALP and ARS staining of after remove of exogenous glutamine in culture medium and rescue effects of 2 mM/4mMDM-αKG. **K** Quantification analysis of ALP and ARS staining using Image J software(Version 1.8.0). (L) qPCR results of ALP and RUNX2

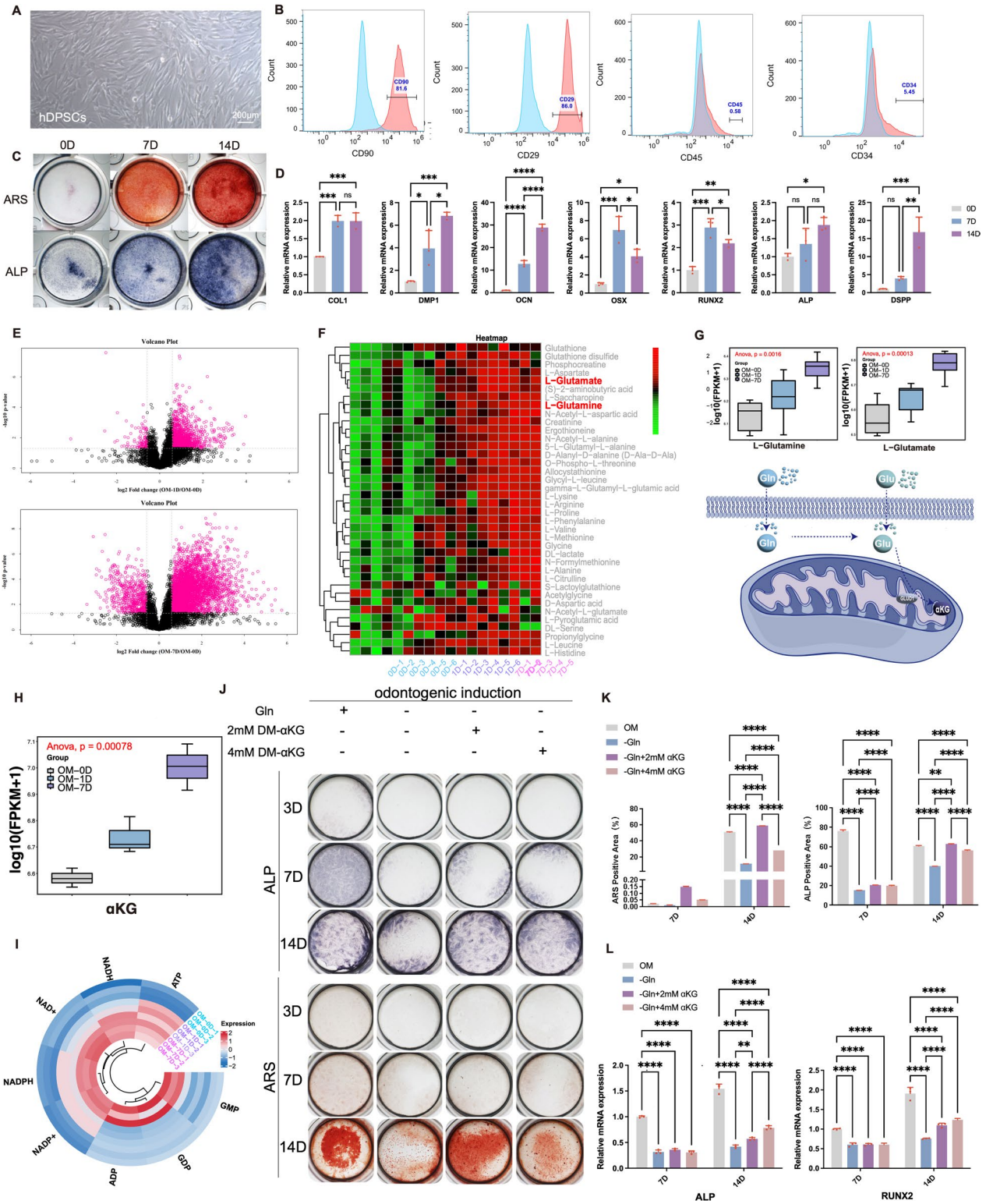

Fig. 1 (See legend on previous page.)

αKG during the osteo/odontogenic differentiation. Since αKG itself cannot penetrate the cell membrane, dimethyl α-ketoglutarate (DM-αKG) was used in this research as a cell permeable derivative of αKG, whose applicability was reported by previous studies [26, 27].The dose-dependent promotive effect of αKG supplementation was confirmed via ARS and ALP staining assay (Fig. 3A), that more Alizarin red positive mineralized nodules and higher ALP activity were detected. Further qPCR results also displayed that under the usage of 2 mM DM-αKG supplementation could upregulate the expression of COL1, OCN, OSX and RUNX2, especially OSX during early osteo/odontogenic differentiation (D7 after induction), while 4 mM DM-αKG seemed to have no better promoting effect (Fig. 3B), and this is also the reason to choose to use 2 mM DM-αKG and focus on early differentiation for follow-up experiments.

Glutamine-derived αKG elimination via GLUD1 knockdown inhibits osteo/odontogenic differentiation and proliferation of hDPSCs

GLUD1 is a key enzyme that catalyzed glutamate into αKG. Immunochemistry displayed that Glud1/2 was highly expressed in mature odontoblast (Fig. 4A^{c}) in mice incisor and deficient in ameloblast (Fig. 4A^{d}), indicating its vital role in osteo/odontogenic differentiation. We further confirmed that GLUD1/2 displayed upregulation of both protein and mRNA levels in pace with hDPSCs osteo/odontogenic differentiation (Fig. 4B-C) (Full length blots are presented in Additional file 1: Fig. S1). mRNA level of other glutamine-αKG axis related enzymes including GOT1, GOT2, GPT and GPT2 only be upregulated during early differentiation (Additional file 1: Fig. S4A). ShRNA technology was used to construct a lentivirus transfection system to knock down GLUD1 in hDPSCs (Fig. 4D), while the knockdown efficiency was verified via qPCR and western blot (Fig. 4E-F) (Full length blots are presented in Additional file 1: Fig. S1). It's necessary to stress that after the knockdown of GLUD1 in hDPSCs, the concentration of αKG was significantly reduced and can be restored via 2 mM DM-αKG supplementation (Fig. 4G-H). After GLUD1 knockdown, proliferation related marker Ki67 was downregulated and could be rescued on D14 (Additional file 1: Fig. S4B). This is in accordance with cell cycle experiments that in sh-GLUD1 group the G1 phase cell distribution increased while S phase cell distribution decreased and can be rescued by αKG supplementation (Additional file 1: Fig. S4C-D). Sh-GLUD1 group presented less Alizarin red positive mineralized nodules and lower ALP activity, while administration of 2 mM DM-αKG can partially rescue the inhibition of osteo/odontogenic differentiation (Fig. 4I, Additional file 1: Fig. S4E). Meanwhile, the relative mRNA level of osteogenic and osteo/odontogenic related genes including COL1, DMP1, OCN, OSX, RUNX2, ALP and DSPP significantly reduced, and among them DMP1, OCN, ALP and DSPP can be significantly rescued on D7(Fig. 4J) and D14 (Fig. 4K). In general, suppression of GLUD1-mediated glutamine-αKG axis could inhibit osteo/odontogenic differentiation and proliferation ability of hDPSCs.

Glutamine-derived αKG elimination via GLUD1 knockdown can abnormally disturb extracellular matrix function and IGF2 expression

The negative influence on osteo/odontogenic differentiation of GLUD1 was reported before [28], and our aforementioned results further confirmed this point. For deeper exploration, we performed transcriptome sequencing, in which the results showed that extracellular matrix function was significantly affected (Fig. 5A). Gene Ontology (GO) enrichment analysis (AvsK) showed differential genes were enriched in several extracellular functions related processes including extracellular region, extracellular space, collagen-containing extracellular matrix etc. (Fig. 5B). Accordingly, Kyoto Encyclopedia of

(See figure on next page.)

Fig. 2 αKG accelerates the growing speed of mouse clipped incisor and dentin formation around cervical loop. **A** *Ki67* immunostaining comparing clipping-D0 and clipping-D3. LaCL: labial cervical loop; MTACs: mesenchymal transit amplifying cells; NVB: neurovascular bundle. White asterisks indicate *Ki67*$^{-}$ region. White arrows indicate *Ki67*.$^{+}$ DESCs. Dashed lines indicate the outline of LaCL. **B** Diagrammatic sketch of fluorescence double-labeling model using calcein-green, and alizarin-red. **C** Lower incisor was separated intactly under Stereomicroscope. **D** Merged fluorescence picture of CL, in which newly generated dental hard tissue was display by red fluorescence, white arrows marked the timepoint of clipping and calcein injection. **E**, **E'** immunofluorescence staining of *Ki67*. **F** Statistic analysis between control and 0.25%(w/v)αKG group (t-test was performed) ($n=6$ mice per group). **G** Statistic analysis between clipping and non-clipping group (paired t-test was performed) ($n=6$ mice per group). **H** Masson's trichrome staining of labial cervical loop (LaCL) in four groups. The white dashed line indicates the dentin deposition point, while the red dashed line indicates the starting end of LaCL. The distance between two lines was record as D1. **I** Statistic analysis of D1 between groups (unpaired t-test was performed) ($n=6$ mice per group). **J-K** Vickers's hardness test of incisors on incisal region and CL region (One-way ANOVA was performed) ($n=5$ mice per group). **L** Sketch map illustrating the effect of αKG on incisor repairment and cervical loop. Dentin was colored as blue, and enamel was colored as red. LiCL: lingual cervical loop; LaCL: labial cervical loop; TAC: transit amplifying cells. Data are presented as mean ± SD.*$P<0.05$. **$P<0.01$. ****$P<0.0001$

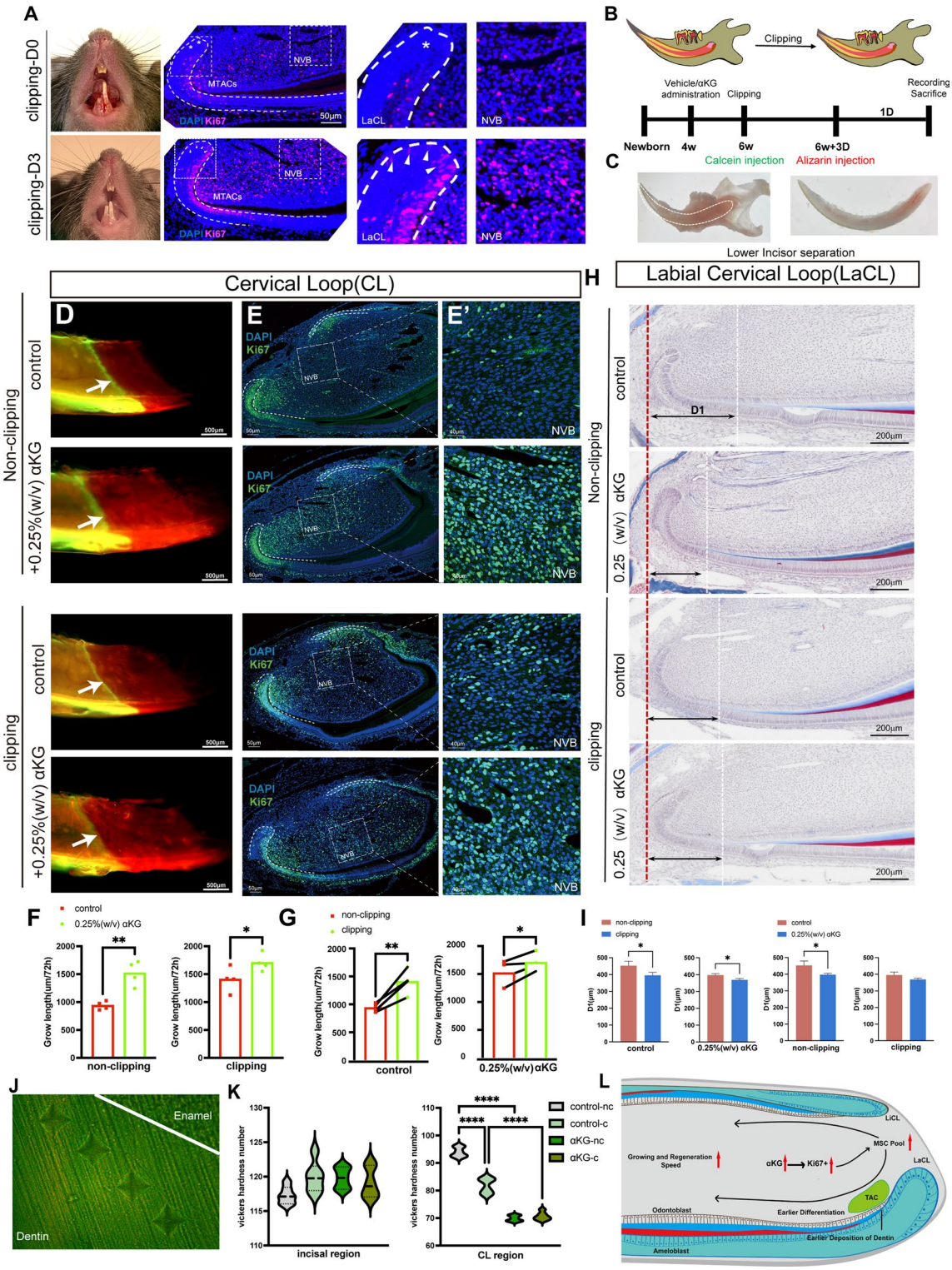

Fig. 2 (See legend on previous page.)

Genes and Genomes (KEGG) enrichment analysis (AvsK) also demonstrated that differential genes were enriched in PI3k-Akt signaling pathway, which is confirmed to be tightly connected with extracellular matrix and environmental information processing (Fig. 5C). We then performed GSEA analysis based on "PI3K-Akt signaling

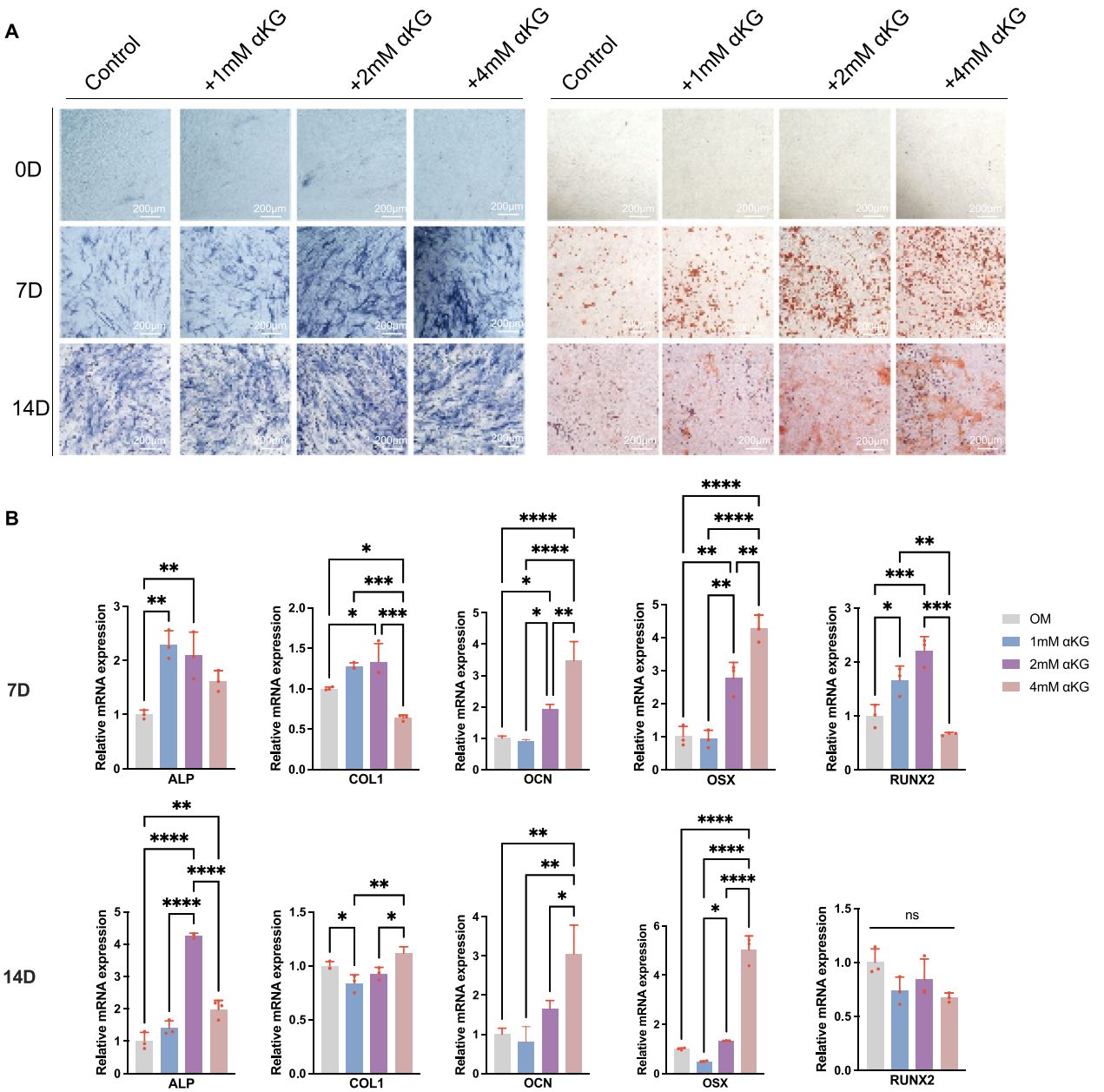

Fig. 3 αKG promotes osteo/odontogenic differentiation of hDPSCs. **A** ALP and ARS staining of hDPSCs cultured in medium supplemented with different concentration of DM-αKG on D0, D7, D14 after osteo/odontogenic differentiation**. B** qPCR results of osteo/odontogenic and osteogenic related genes including ALP, COL1, OCN, OSX and RUNX2 (One-way ANOVA was performed)**.** Data are presented as mean ± SD.*$P < 0.05$. **$P < 0.01$. ****$P < 0.0001$

pathway" gene set and the results confirmed that it was significantly enriched and upregulated in sh + 2 mM αKG group, indicating its potential role in αKG rescue effect after GLUD1 knockdown (Fig. 5D). The top 10 differential significant genes of "AvsK" included FP236383, FP671120, FP236383, FP671120, AC093512, SOST, DIO2, MASP1 and IGF2, which were displayed in volcano plot (Fig. 5E). We then carried out PPI network analysis and acquired top 10 hub genes (HG) including DPP4, IGF2, TFRC, IGFBP5 etc. (Fig. 5F). Via cross-referencing differential genes (DIF), GSEA leading edge genes (LEG) in "PI3k-Akt signaling pathway" gene set and hub genes (HG) in "AvsK" comparing group, two genes including IGF2 and THBS2 were screened out

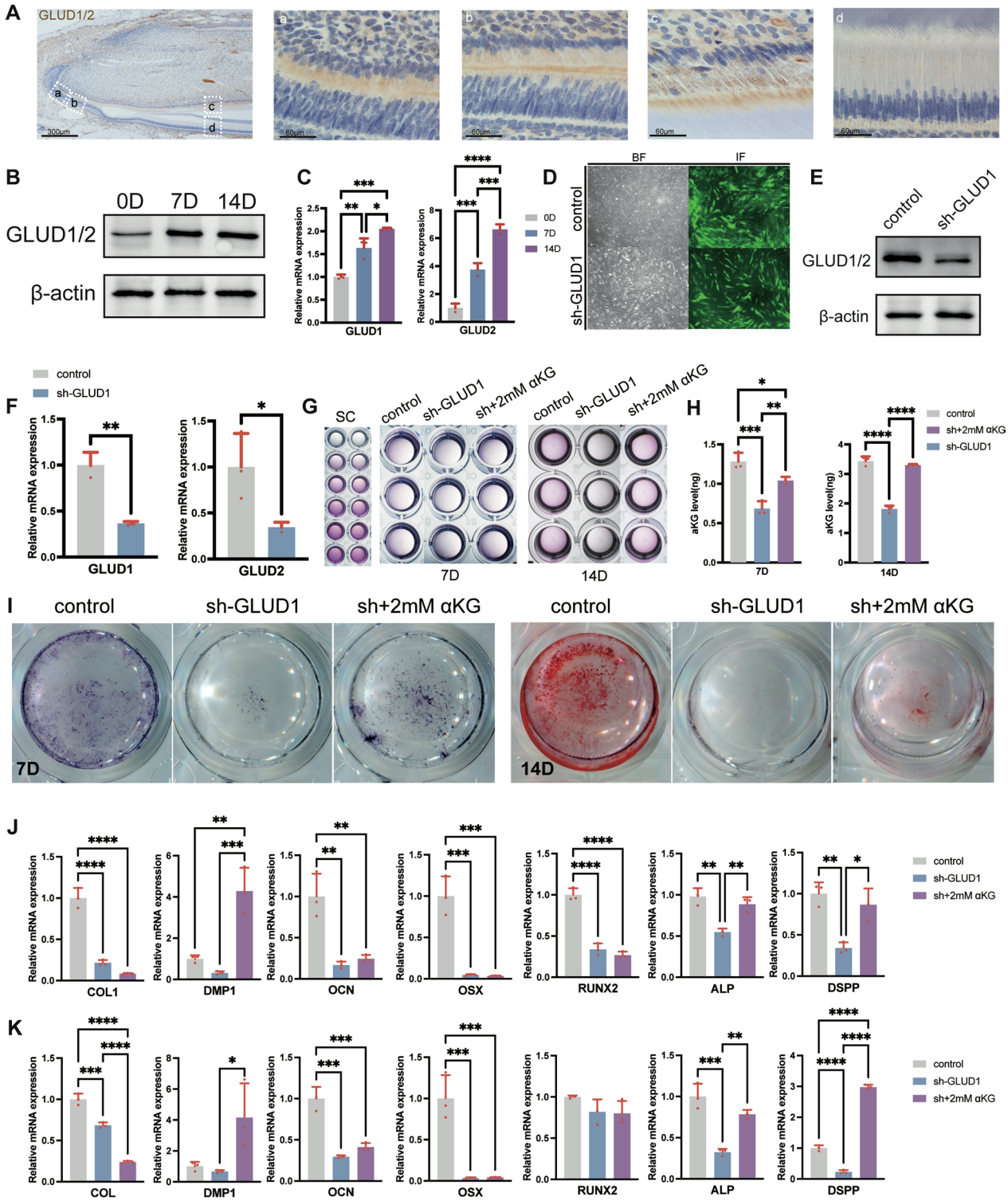

Fig. 4 αKG elimination could inhibit osteo/odontogenic differentiation. **A** Immunochemistry staining of *Glud1/2*. a: pre-odontoblast; b: presecretory odontoblast; c: secretory odontoblast; d: secretory ameloblast. **B-C** The increasing expression tendency of GLUD1 during osteo/odontogenic differentiation. **D-F** Knockdown of GLUD1 using shRNA technique. **G-H** αKG level evaluation via colorimetric assay (One-way ANOVA was performed). **I** ALP and ARS staining of control, shGLUD1 and sh + 2 mM αKG group. **J-K** qPCR results of **osteo/odontogenic** related genes including COL1, DMP1, OCN, OSX, RUNX2, ALP and DSPP on D7 and D14 respectively (One-way ANOVA was performed). Data are presented as mean ± SD.*$P < 0.05$. **$P < 0.01$. ****$P < 0.0001$

(Fig. 5G). Further qPCR verification displayed that IGF2 was significantly downregulated after GLUD1 knockdown and was significantly rescued by αKG supplementation (Fig. 5H). Immunocytochemistry and qPCR also displayed that exogenous αKG could significantly promote the expression of IGF2 in hDPSCs (Fig. 5I-J). Above results indicated the involvement of IGF2 in this GLUD1-involved glutamine-αKG axis.

Glutamine-derived αKG elimination influenced translation efficiency of IGF2 via m6A modification

Glutamine metabolism was reported to be actively regulated by m6A methylation modification [29–32], while IGF2BPs were also reported as m6A "writers." To investigate if the m6A modification was disturbed under the circumstance of glutamine-αKG axis suppression, we firstly measured the total m6A methylation level when exogenous glutamine was eliminated, in which total m6A methylation level was downregulated (Fig. 6B). Consistently, we also observed a significant decline of total m6A methylation level in sh-GLUD1, while supplementation of exogenous αKG can rescue the downregulation (Fig. 6C). MeRIP-qPCR showed the relative m6A methylation enrichment of IGF2 in sh-GLUD1 was significantly reduced compared with control group, while exogenous αKG could significantly rescue the inhibition (Fig. 6D-E). Since m6A modification has been widely studied to be able to regulate gene expression by either affecting RNA stability [33] or translation efficiency [34], we confirmed that both mRNA level and protein enrichment of IGF2 decreased in sh-GLUD1 group and could be rescued by αKG supplementation (Figs. 5H, 6F) (Full length blots are presented in Additional file 1: Fig. S1). Further, suppressed IGF2 translation efficiency was observed in sh-GLUD1 group and can be rescued in sh + 2 mM αKG group (Fig. 6G-H). Above results indicated that glutamine-αKG axis may affect odontogenesis differentiation of human dental pulp stem cells via suppressing IGF2 translation efficiency in a m6A-modification-involved way. The illustration of regulation mechanism was displayed as graphic (Fig. 7).

Discussion

In the process of glutamine metabolism to generate αKG, GLUD1 is a mitochondrial enzyme and meditate one of the most canonical glutamine-αKG axis pathway. Lin and colleagues [35] have verified the promoting effect of GLUD1 on αKG accumulation and mTOR signaling pathway activation, which may finally lead to myocardial hypertrophy. According to Brown and colleagues [36], overexpression of GLUD1 in BMMSCs could promote the conversion of glutamate to α-KG in enteric nervous system (ENS) injury microenvironment, thereby increasing histone demethylation of H3K9 and H3K27, promoting the differentiation of bone marrow mesenchymal stem cells (BMMSCs). In this paper, since intracellular αKG level is hard to be directly intervened, confirming the influence of GLUD1 knockdown on αKG level is critical. Cheerfully and importantly, our results confirmed that GLUD1 knockdown can indeed reduce the intracellular αKG level of hDPSCs, which provide us a solid foundation for subsequent experiments.

As our RNA-seq data displayed, the effect of GLUD1 knockdown or αKG supplementation mainly centered on ECM, which was described as a dynamic and complex environment owning biophysical, mechanical and biochemical properties specific for each tissue and able to regulate cell behavior [37],as well as high application potential or studying value in tissue engineering [38]. The GO analysis provided adequate evidence that extracellular region was actively involved in αKG supplementation and elimination, and the KEGG analysis pointed out the involvement of PI3k-Akt signaling pathway, while further GSEA analysis and PPT network analysis led us to the hypothesis of IGF2 involvement in glutamine-αKG axis related dentinogenesis process. PI3k-Akt signaling pathway is an intracellular signal transduction pathway that positively responds to ECM signals, regulates ECM remodeling, affects cell metabolism, proliferation, survival, growth, and even angiogenesis [39]. IGF2 is member of PI3k-Akt signaling pathway and an imprinted gene with structural and regulatory complexity, with pleiotropy, tissue specificity and developmental stage dependence [40], associated with several diseases like cancer,

(See figure on next page.)

Fig. 5 Glutamine-derived αKG elimination via GLUD1 knockdown can abnormally disturb extracellular matrix function and IGF2 expression. **A** Sketch map of target gene screening. **B**–**C** Scatter plot of GO and KEGG analysis comparing sh-GLUD1 and sh + 2 mM αKG group (AvsK), in which the red-highlighted indicated differential genes were enriched in extracellular-related functions and PI3k-Akt signaling pathway. Enriched gene number was displayed by circle size, while the enrichment significance was displayed by different color according to the color bar on the right side. **D** GSEA analysis of PI3k-Akt signaling pathway comparing "AvsK". **E** Volcano plot of differential genes comparing "AvsK". **F** PPI network analysis comparing "AvsK", and top 10 hub genes analyzed by Cytoscape Software Ver.3.8.2 were displayed and ranked. **G** Venn plot displaying cross filtering of differential genes, GSEA leading edge genes (LEG) in PI3k-Akt signaling pathway gene set and PPI network top 10 hub genes comparing "AvsK". **H–I** qPCR verification of potential key gene-IGF2. **J** Immunocytochemistry staining of IGF2 comparing in control and 2 mM αKG group. Data are presented as mean ± SD.*$P < 0.05$. **$P < 0.01$. ****$P < 0.0001$

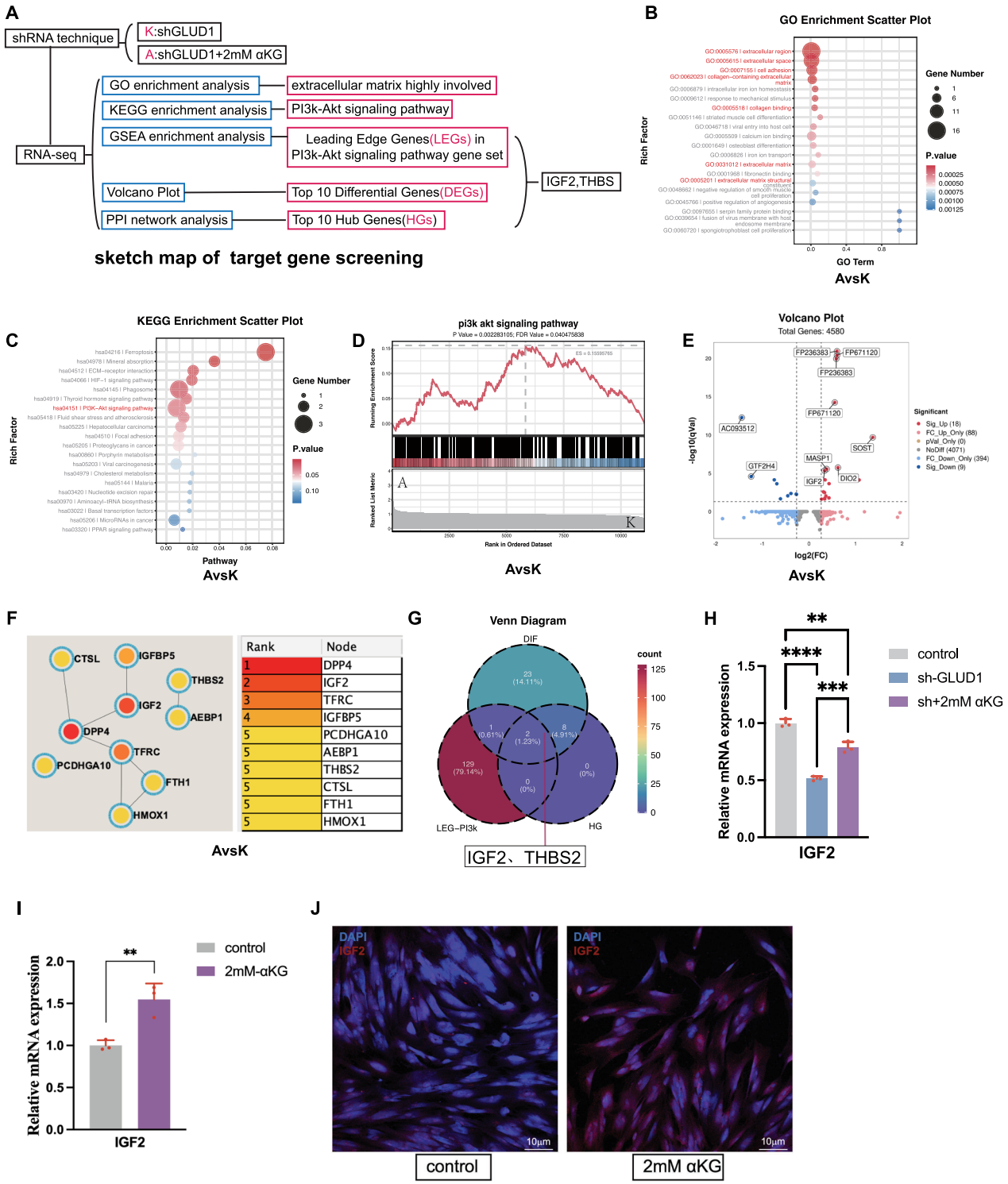

Fig. 5 (See legend on previous page.)

neurodevelopmental disorders [41],bone-related diseases [42] and signaling pathways like sonic hedgehog (Shh), PI3K/Akt [42], BMP [43] signaling pathway etc. It is worth noting that, IGF family and IGF2 are closely related to ECM function [44] and glutamine-αKG axis [12]. More importantly, IGF2 involvement was revealed

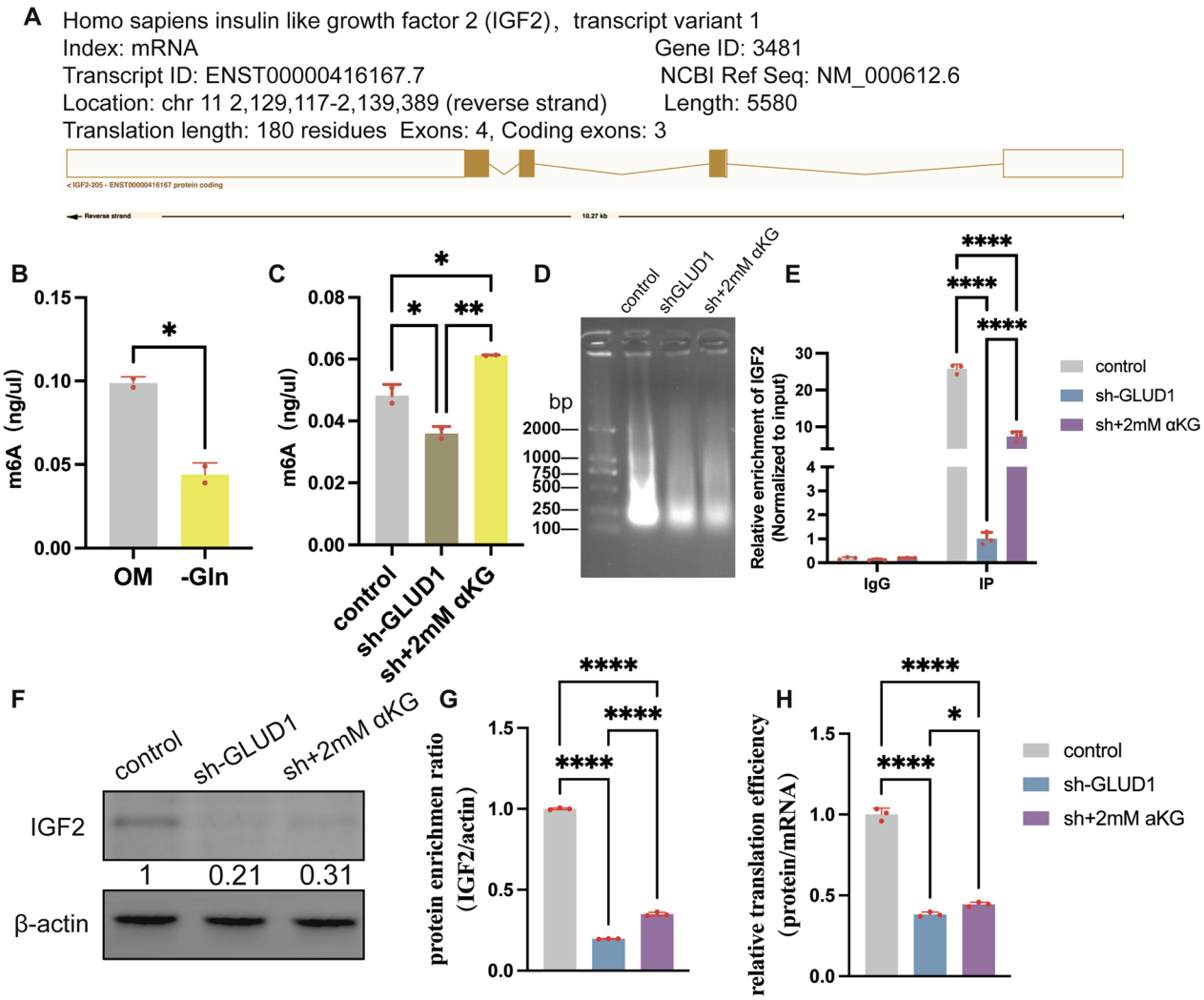

Fig. 6 αKG elimination influenced translation efficiency of IGF2 via m6A modification. **A** Details of IGF2 mRNA transcript used for primer design. **B–C** m6A level evaluation using calorimetric assay (Cat. #P-9005, Epigentek, USA) (One-way ANOVA was performed). **D-E** MeRIP-qPCR of IGF2, the enrichment was normalized to input (One-way ANOVA was performed). **F** Western Blot of IGF2 in control, shGLUD1 and sh + 2 mM αKG group. **G** Relative quantification of western blot using ImageJ software (One-way ANOVA was performed). **H** Relative translation efficiency of IGF2 (One-way ANOVA was performed)

in tooth development. Al-Khafaji and colleagues [45] reported that increased expression of IGF2 under osteogenic conditions of human dental pulp cells. Chen and colleagues [46] uncovered a cascade Runx2-IGF signaling network in the MSC niche of the adult mouse incisor, that exogenous Igf2 could rescue MSC proliferation and odontoblast differentiation defects in incisors of adult Runx2 mutant mice, where the IGF downstream targets p-Irs1 and p-Akt were downregulated.

It is reported IGF2BPs as a distinct family of m6A readers that able to regulate gene expression in an m6A-depedent manner [30, 32, 33, 47]. m6A methylation refers to as one of the most prevalent and abundant mRNA epigenetic modification [48–50], which was widely proved to be associated with life activities like organ development [49], tumorigenesis, bone homeostasis [51], metabolism [47, 52], and is also an important regulatory mechanism in determining the fate of stem cells [20, 21, 33, 48, 53]. According to current research, m6A modifications could take part in dynamic mRNA metabolism via affecting RNA stability and translation efficiency [34, 47]. As for m6A methylation in DPSCs, m6A methylation has been reported to present a unique enhanced pattern during dentinogenesis differentiation recently [54]. Luo and colleagues [55] revealed that m6A methylated hallmarks in DPSCs and a regulatory role of

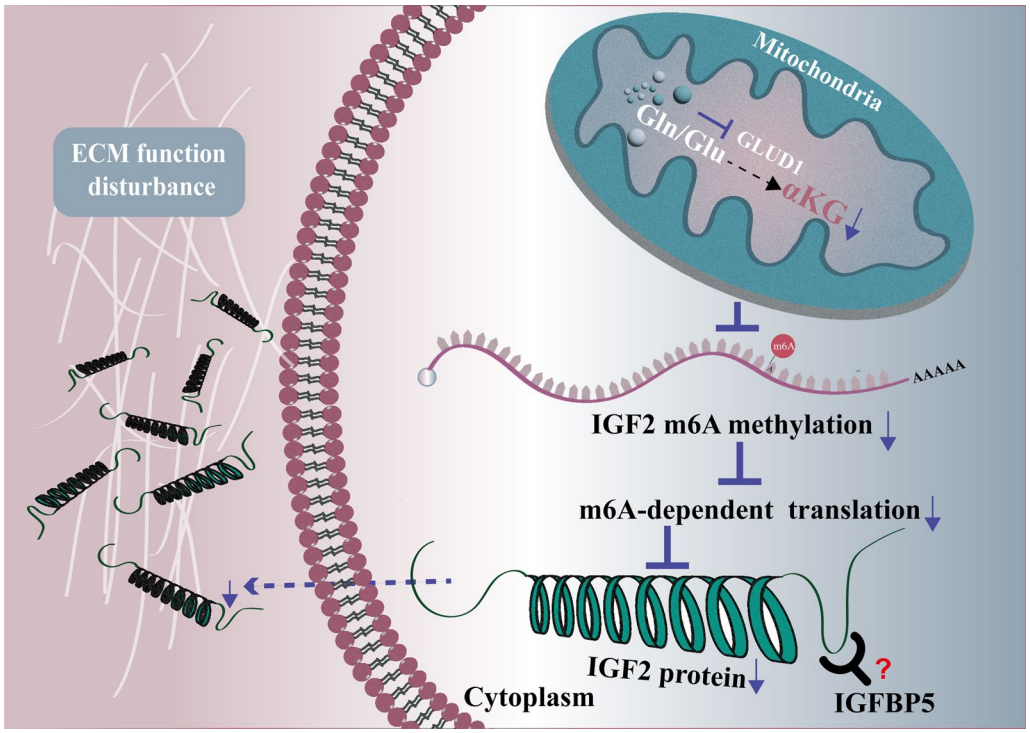

Fig. 7 Sketch map of research illustration

METTL3 in cell cycle control of hDPSCs. More importantly, the relationship between IGFs and m6A methylation was gradually revealed recently as well. According to our results, after glutamine-αKG axis suppression via GLUD1 knockdown, differential genes enriched in PI3K-Akt signaling pathway, while hDPSCs osteo/odontogenic differentiation and IGF2 m6A methylation were both significantly inhibited. This is in accordance with Tian and colleagues' research [56]. We also noticed that according to our PPI network analysis, IGF2 may highly interacted with IGFBP5, which could be further explored to find out whether IGFBP5 was involved in m6A modification as one of IGFBPs. The molecular docking model of IGF2 and IGFBP5 was displayed in Additional file 1: Fig. S5.

Cervical loop (CL) refers to the special structure at the distal end of rodents' incisor, which is the main reason of its lifelong sustained growth [23, 46, 57]. Explored by massive research [24, 25], there are sufficient rationality to believe that cervical loop and its interaction with mesenchyme might be the key structure and reason of constant growing of rodent incisors. Ki67 was used to observe dental mesenchymal of Stat3 CKO mice [58] and epithelial–mesenchymal interactions between mesenchymal transit amplifying cells (MTACs) and CL-MSCs during tooth wound healing [25]. In this paper, we found Ki67-positive cell number and region area significantly increased in αKG application group and clipping group compared to control, especially in MSC region, suggesting activated MSCs and the expansion of MSC pool. To evaluate the effect of αKG on hard tissue regeneration, we found that exogenous αKG can accelerate the growing and repairing speed of rodent incisors via an incisor clipping and fluorescence double-labeling animal model described in 2.7. Further, we specifically observed the blue-dyed dentin through Masson's Trichrome Staining Assay [23] and found out dentin deposition start point moved forward towards cervical loop in αKG group, indicating that the dentin formation was promoted, and the differentiation was brought to an early point.

The superiority and particularity of αKG to be explored as a potential stem cell therapy drug is its metabolite identity. Compared to synthetic drugs, αKG is natural and has higher biosafety, and there is also an αKG-based formula medicine called "Rejuvant", claiming it can "delay the aging process." Demidenko and colleagues [59] conducted a retrospective study of 42 participants who took "Rejuvant" for about 7 months and found that it can indeed reduce the physiological age of the users. The explanation of αKG can be multifaceted, since that cell proliferation, cell differentiation, matrix secretion and matrix mineralization might all get involved during the process. Further discoveries and profound literatures are still needed to dig deeper into the secret connection of metabolism, epigenetics, and dental tissue regeneration.

Conclusion

Adult stem cells (ASCs) are essential for tissue engineering and regeneration, while dental pulp derived mesenchymal adult stem cells (m-ASCs), so called hDPSCs in this research, displayed significant superiority of easy accessibility and typical pluripotent ability. This research explored the epigenetic-metabolism mechanism of glutamine-αKG axis during the differentiation of hDPSCs, meanwhile provided new insights into metabolite-based drug development for tissue regeneration and repairment.

Abbreviations

m-ASCs	Mesenchymal adult stem cells
hDPSCs	Human dental pulp cells
GLUD1	Glutamate dehydrogenase 1
GPT	Glutamate-pyruvate transaminase
GOT	Glutamic-oxaloacetic transaminase
ECM:	Extracellular matrix
IGF2	Insulin-like growth factor 2
GLS	Glutaminase
METTL3	Methyltransferase-like 3
ARS	Alizarin red S
ALP	Alkaline phosphatase
COL1	Collagen type I
DMP1	Dentin matrix acidic phosphoprotein 1
OCN	Osteocalcin
OSX	Osterix
RUNX2	Runt related transcription factor 2
DSPP	Dentin sialophosphoprotein
NAD /NADH	Nicotinamide adenine dinucleotide
NADP /NADPH	Nicotinamide adenine dinucleotide phosphate
ADP	Adenosine diphosphate
ATP	Adenosine triphosphate
CL	Cervical loop
LaCL	Labial cervical loop
MTACs	Mesenchymal transit amplifying cells
NVB	Neurovascular bundle
LiCL	Lingual cervical loop
DM-αKG	Dimethyl α-ketoglutarate
αKG	α-ketoglutarate
GO	Gene Ontology
KEGG	Kyoto Encyclopedia of Genes and Genomes

Supplementary Information

The online version contains supplementary material available at https://doi.org/10.1186/s13287-024-04092-6.

Additional file 1. Supplemental Figures.

Additional file 2. Primers of RT-qPCR and MeRIP-qPCR.

Acknowledgements

We are here thankful for West China Hospital of Stomatology of Sichuan University State Key Laboratory of Oral Diseases & National Clinical Research Center for Oral Diseases providing facilities.

Author contributions

Yachuan Zhou and Liwei Zheng performed study concept and design; Qinglu Tian and Yachuan Zhou performed development of methodology and writing, review, and revision of the paper; Qinglu Tian and Shiqi Gao provided acquisition, analysis and interpretation of data, and statistical analysis; Siying Li, Mian Wan, Xin Zhou and Xuedong Zhou provided technical and material support. All authors read and approved the final paper. All authors should agree to be accountable for all aspects of the work to ensure that the questions related to the accuracy or integrity of any part of the work are appropriately investigated and resolved.

Funding

This work was supported by the National Natural Science Foundation of China (NSFC) Grant (No. 81800927) to Yachuan Zhou and National Natural Science Foundation of China (NSFC) Grant (No. 82170921) to Liwei Zheng.

Availability of data and materials

The datasets used and analyzed during the current study are available from the corresponding author on reasonable request. RNA-seq raw data are available at the BioProject database under accession number PRJNA1157584. Metabolomics raw data are available at the Metabolight database under accession number MTBLS11058.

Declarations

Ethics approval and consent to participate

Our studies include human resource dental pulp stem cells and animal studies was approved as followed detail. (1) Title of the approved project: The potential epigenetic mechanism of glutamate metabolism and αKG regulating dental pulp stem cell differentiation; (2) Name of the institutional approval committee: Ethics Committee of West China School of Stomatology, Sichuan University; (3) Approval number: No. WSHSIRB- D-2022-519(for human dental pulp stem cells) and NO.WSHSIRB-D-2022-669(for mouse experiments); (4) Date of approval: 2022.12.15. The patients provided written informed consent for the use of extracted human teeth samples for cell culture and further research. All samples were extracted due to medical needs. The procedure of cell isolation and cultivation was described in "Methods".

Consent for publication

Not applicable.

Competing interests

All authors declare that there are no competing interests regarding the publication of this paper.

Author details

[1]State Key Laboratory of Oral Diseases, National Clinical Research Center for Oral Diseases, Department of Pediatric Dentistry, West China Hospital of Stomatology, Sichuan University, Chengdu 610041, Sichuan, China. [2]State Key Laboratory of Oral Diseases, National Clinical Research Center for Oral Diseases, Department of Cariology and Endodontics, West China Hospital of Stomatology, Sichuan University, Chengdu 610041, Sichuan, China. [3]Department of Pediatric Dentistry, School and Hospital of Stomatology, Guangdong Engineering Research Center of Oral Restoration and Reconstruction & Guangzhou Key Laboratory of Basic and Applied Research of Oral Regenerative Medicine, Guangzhou Medical University, Guangzhou, China.

Received: 6 September 2024 Accepted: 4 December 2024
Published online: 18 December 2024

References

1. Zhao J, Du W, Guo D, Wang S, Du W. Mechanical signaling in dental pulp stem cells. Front Biosci (Landmark Ed). 2023;28(10):274.
2. Nagata M, Ono N, Ono W. Unveiling diversity of stem cells in dental pulp and apical papilla using mouse genetic models: a literature review. Cell Tissue Res. 2021;383(2):603–16.
3. Ferro F, Spelat R, Baheney CS. Dental pulp stem cell (DPSC) isolation, characterization, and differentiation. Methods Mol Biol. 2014;1210:91–115.
4. Tsutsui TW. Dental pulp stem cells: advances to applications. Stem Cells Cloning. 2020;13:33–42.
5. Yang X, Li L, Xiao L, Zhang D. Recycle the dental fairy's package: overview of dental pulp stem cells. Stem Cell Res Ther. 2018;9(1):347.
6. Luo N, Deng YW, Wen J, Xu XC, Jiang RX, Zhan JY, et al. Wnt3a-loaded hydroxyapatite Nanowire@Mesoporous silica core-shell nanocomposite promotes the regeneration of dentin-pulp complex via

angiogenesis, oxidative stress resistance, and odontogenic induction of stem cells. Adv Healthc Mater. 2023;12(22):e2300229.
7. Han J, Kim DS, Jang H, Kim HR, Kang HW. Bioprinting of three-dimensional dentin-pulp complex with local differentiation of human dental pulp stem cells. J Tissue Eng. 2019;10:2041731419845849.
8. Xiao D, Zeng L, Yao K, Kong X, Wu G, Yin Y. The glutamine-alpha-ketoglutarate (AKG) metabolism and its nutritional implications. Amino Acids. 2016;48(9):2067–80.
9. Liu S, He L, Yao K. The antioxidative function of alpha-ketoglutarate and its applications. Biomed Res Int. 2018;2018:3408467.
10. Wu N, Yang M, Gaur U, Xu H, Yao Y, Li D. Alpha-ketoglutarate: physiological functions and applications. Biomol Ther (Seoul). 2016;24(1):1–8.
11. Stanley CA, De Léon DD. Amino acid-stimulated insulin secretion: the role of the glutamine-glutamate-alpha-ketoglutarate axis. Front Diabetes. 2012;12:112–24.
12. Li C. Insulin secretion and the glutamine-glutamate-alpha-ketoglutarate axis. New York: Springer; 2015.
13. Lee S, Kim HS, Kim MJ, Min KY, Choi WS, You JS. Glutamine metabolite α-ketoglutarate acts as an epigenetic co-factor to interfere with osteoclast differentiation. Bone. 2021;145:115836.
14. Wang Y, Deng P, Liu Y, Wu Y, Chen Y, Guo Y, et al. Alpha-ketoglutarate ameliorates age-related osteoporosis via regulating histone methylations. Nat Commun. 2020;11(1):5596.
15. Carey BW, Finley LW, Cross JR, Allis CD, Thompson CB. Intracellular α-ketoglutarate maintains the pluripotency of embryonic stem cells. Nature. 2015;518(7539):413–6.
16. Uribe-Etxebarria V, Agliano A, Unda F, Ibarretxe G. Wnt signaling reprograms metabolism in dental pulp stem cells. J Cell Physiol. 2019;234(8):13068–82.
17. Choi B, Kim JE, Park SO, Kim EY, Oh S, Choi H, et al. Sphingosine-1-phosphate hinders the osteogenic differentiation of dental pulp stem cells in association with AKT signaling pathways. Int J Oral Sci. 2022;14(1):21.
18. Wang K, Zhou L, Mao H, Liu J, Chen Z, Zhang L. Intercellular mitochondrial transfer alleviates pyroptosis in dental pulp damage. Cell Prolif. 2023;56(9):e13442.
19. Ren R, Ocampo A, Liu GH, Izpisua Belmonte JC. Regulation of stem cell aging by metabolism and epigenetics. Cell Metab. 2017;26(3):460–74.
20. Ermolaeva M, Neri F, Ori A, Rudolph KL. Cellular and epigenetic drivers of stem cell ageing. Nat Rev Mol Cell Biol. 2018;19(9):594–610.
21. Liang G, Zhang Y. Embryonic stem cell and induced pluripotent stem cell: an epigenetic perspective. Cell Res. 2013;23(1):49–69.
22. Ching HS, Luddin N, Rahman IA, Ponnuraj KT. Expression of odontogenic and osteogenic markers in DPSCs and SHED: a review. Curr Stem Cell Res Ther. 2017;12(1):71–9.
23. Yu F, Li F, Zheng L, Ye L. Epigenetic controls of Sonic hedgehog guarantee fidelity of epithelial adult stem cells trajectory in regeneration. Sci Adv. 2022;8(29):eabn4977.
24. An Z, Sabalic M, Bloomquist RF, Fowler TE, Streelman T, Sharpe PT. A quiescent cell population replenishes mesenchymal stem cells to drive accelerated growth in mouse incisors. Nat Commun. 2018;9(1):378.
25. Walker JV, Zhuang H, Singer D, Illsley CS, Kok WL, Sivaraj KK, et al. Transit amplifying cells coordinate mouse incisor mesenchymal stem cell activation. Nat Commun. 2019;10(1):3596.
26. Wang Z, Hu J, Faber J, Miszuk J, Sun H. Locally delivered metabolite derivative promotes bone regeneration in aged mice. ACS Appl Bio Mater. 2022;5(7):3281–9.
27. Tatara MR, Pierzynowski GS, Majcher P, Krupski W, Wawrzyniak-Gacek A, Filip R, et al. The influence of alpha-ketoglutarate (AKG) on mineralisation, mechanical and structural properties of ulna in turkey under conditions of osteotomy and denervation. Ortop Traumatol Rehabil. 2003;5(5):666–72.
28. Lu X, Liu S, Zhao S. Effect of GLUD1 on proliferation, osteogenic differentiation and mineralization of human dental pulp stem cells. Shanghai J Stomatol. 2017;26(4):358–62.
29. Zhao L, Guo J, Xu S, Duan M, Liu B, Zhao H, et al. Abnormal changes in metabolites caused by m(6)A methylation modification: The leading factors that induce the formation of immunosuppressive tumor microenvironment and their promising potential for clinical application. J Adv Res. 2024;3:69.
30. Weng H, Huang F, Yu Z, Chen Z, Prince E, Kang Y, et al. The m(6)A reader IGF2BP2 regulates glutamine metabolism and represents a therapeutic target in acute myeloid leukemia. Cancer Cell. 2022;40(12):1566-82.e10.
31. Sun S, Gao T, Pang B, Su X, Guo C, Zhang R, et al. RNA binding protein NKAP protects glioblastoma cells from ferroptosis by promoting SLC7A11 mRNA splicing in an m(6)A-dependent manner. Cell Death Dis. 2022;13(1):73.
32. Zhou T, Xiao Z, Lu J, Zhang L, Bo L, Wang J. IGF2BP3-mediated regulation of GLS and GLUD1 gene expression promotes treg-induced immune escape in human cervical cancer. Am J Cancer Res. 2023;13(11):5289–305.
33. Huang H, Weng H, Sun W, Qin X, Shi H, Wu H, et al. Recognition of RNA N(6)-methyladenosine by IGF2BP proteins enhances mRNA stability and translation. Nat Cell Biol. 2018;20(3):285–95.
34. Wang X, Zhao BS, Roundtree IA, Lu Z, Han D, Ma H, et al. N(6)-methyladenosine modulates messenger RNA translation efficiency. Cell. 2015;161(6):1388–99.
35. Lin ZR, Li ZZ, Cao YJ, Yu WJ, Ye JT, Liu PQ. GDH promotes isoprenaline-induced cardiac hypertrophy by activating mTOR signaling via elevation of α-ketoglutarate level. Naunyn Schmiedebergs Arch Pharmacol. 2022;395(11):1373–85.
36. Fan M, Shi H, Yao H, Wang W, Zhang Y, Jiang C, et al. Glutamate regulates gliosis of BMSCs to promote ENS regeneration through α-KG and H3K9/H3K27 demethylation. Stem Cell Res Ther. 2022;13(1):255.
37. Joo S, Yeon Kim J, Lee E, Hong N, Sun W, Nam Y. Effects of ECM protein micropatterns on the migration and differentiation of adult neural stem cells. Sci Rep. 2015;5:13043.
38. Saraswathibhatla A, Indana D, Chaudhuri O. Cell-extracellular matrix mechanotransduction in 3D. Nat Rev Mol Cell Biol. 2023;24(7):495–516.
39. Li X, Pan J, Liu T, Yin W, Miao Q, Zhao Z, et al. Novel TCF21(high) pericyte subpopulation promotes colorectal cancer metastasis by remodelling perivascular matrix. Gut. 2023;72(4):710–21.
40. DeChiara TM, Robertson EJ, Efstratiadis A. Parental imprinting of the mouse insulin-like growth factor II gene. Cell. 1991;64(4):849–59.
41. Alberini CM. IGF2 in memory, neurodevelopmental disorders, and neurodegenerative diseases. Trends Neurosci. 2023;46(6):488–502.
42. Hamamura K, Zhang P, Yokota H. IGF2-driven PI3 kinase and TGFbeta signaling pathways in chondrogenesis. Cell Biol Int. 2008;32(10):1238–46.
43. Chen L, Jiang W, Huang J, He BC, Zuo GW, Zhang W, et al. Insulin-like growth factor 2 (IGF-2) potentiates BMP-9-induced osteogenic differentiation and bone formation. J Bone Miner Res. 2010;25(11):2447–59.
44. Lin H, Tian S, Peng Y, Wu L, Xiao Y, Qing X, et al. IGF signaling in intervertebral disc health and disease. Front Cell Dev Biol. 2021;9:817099.
45. Al-Khafaji H, Noer PR, Alkharobi H, Alhodhodi A, Meade J, El-Gendy R, et al. A characteristic signature of insulin-like growth factor (IGF) axis expression during osteogenic differentiation of human dental pulp cells (hDPCs): potential co-ordinated regulation of IGF action. Growth Horm IGF Res. 2018;42–43:14–21.
46. Chen S, Jing J, Yuan Y, Feng J, Han X, Wen Q, et al. Runx2+ niche cells maintain incisor mesenchymal tissue homeostasis through IGF signaling. Cell Rep. 2020;32(6):108007.
47. Wang Y, Wang Y, Gu J, Su T, Gu X, Feng Y. The role of RNA m6A methylation in lipid metabolism. Front Endocrinol (Lausanne). 2022;13:866116.
48. He PC, Wei J, Dou X, Harada BT, Zhang Z, Ge R, et al. Exon architecture controls mRNA m(6)A suppression and gene expression. Science. 2023;379(6633):677–82.
49. Roundtree IA, Evans ME, Pan T, He C. Dynamic RNA modifications in gene expression regulation. Cell. 2017;169(7):1187–200.
50. Holliday R. The inheritance of epigenetic defects. Science. 1987;238(4824):163–70.
51. Huang M, Xu S, Liu L, Zhang M, Guo J, Yuan Y, et al. m6A methylation regulates osteoblastic differentiation and bone remodeling. Front Cell Dev Biol. 2021;9:783322.
52. Cai W, Ji Y, Han L, Zhang J, Ni Y, Cheng Y, et al. METTL3-dependent glycolysis regulates dental pulp stem cell differentiation. J Dent Res. 2022;101(5):580–9.
53. Frye M, Harada BT, Behm M, He C. RNA modifications modulate gene expression during development. Science. 2018;361(6409):1346–9.
54. Pan Y, Liu Y, Cui D, Yu S, Zhou Y, Zhou X, et al. METTL3 enhances dentinogenesis differentiation of dental pulp stem cells via increasing GDF6 and STC1 mRNA stability. BMC Oral Health. 2023;23(1):209.

55. Luo H, Liu W, Zhang Y, Yang Y, Jiang X, Wu S, et al. METTL3-mediated m(6)A modification regulates cell cycle progression of dental pulp stem cells. Stem Cell Res Ther. 2021;12(1):159.
56. Tian C, Huang Y, Li Q, Feng Z, Xu Q. Mettl3 regulates osteogenic differentiation and alternative splicing of vegfa in bone marrow mesenchymal stem cells. Int J Mol Sci. 2019;20(3):36.
57. Pei F, Ma L, Jing J, Feng J, Yuan Y, Guo T, et al. Sensory nerve niche regulates mesenchymal stem cell homeostasis via FGF/mTOR/autophagy axis. Nat Commun. 2023;14(1):344.
58. Chan L, Lu J, Feng X, Lin L, Yao Y, Zhang X. Loss of Stat3 in Osterix(+) cells impairs dental hard tissues development. Cell Biosci. 2023;13(1):75.
59. Demidenko O, Barardo D, Budovskii V, Finnemore R, Palmer FR, Kennedy BK, et al. Rejuvant®, a potential life-extending compound formulation with alpha-ketoglutarate and vitamins, conferred an average 8 year reduction in biological aging, after an average of 7 months of use, in the TruAge DNA methylation test. Aging (Albany NY). 2021;13(22):24485–99.

Publisher's Note